

# Boiling Assemblages in the Kupel Occurrence, Krumovgrad Goldfield, SE Bulgaria

Irina Marinova \* and Elena Tacheva

Institute of Mineralogy and Crystallography, Bulgarian Academy of Sciences; tacheva\_e@abv.bg

\* Correspondence: irimari@gmail.com; Tel.: +359-288-545-3470

**Abstract:** This paper presents a study on boiling assemblages in the Kupel occurrence, as boiling was evidenced by the presence of vein adularia and platy calcite. Fluid inclusion evidence is not available since the present fluid inclusions are very small in size for investigation under optical microscope. Boiling assemblages occur in two types of auriferous mineralization hosted by supradetachment, grey fine-grained arkosic sandstones and presented by (i) veinlets of quartz-adularia and (ii) veinlets of platy calcite. In quartz-adularia veinlets micron-sized electrum aggregates form globular shapes, which reach 800  $\mu\text{m}$  across and are arranged along the veinlet length. In cross-sections electrum aggregates display abundant silicate-filled pores of a few microns in size. Globular geometry of the electrum aggregates and their arrangement along the veinlet length suggest collectively that these globules were flowing particles–flocs but not colloidal particles since the latter are much smaller. In these veinlets electrum is intergrown with micron-sized chalcopyrite, galena, hessite and greenockite. The auriferous calcite veinlets are formed later than the auriferous quartz-adularia ones, since the first clearly has intersected or brecciated the latter. Electrum in the calcite veinlets forms accumulations only in portions of sharp thickness expansions after throttle portions, which are barren. This suggests that electrum has been transported by a flowing fluid, in a particulate form and deposited due to pressure drop during hydrofracturing, as the electrum particles have been arrested in low velocity (expanded) portions of ore conduits. The auriferous assemblages in the Kupel occurrence indicate high effectiveness of boiling for deposition of Au, Ag, Cu, Pb, Cd and Te through collective loss of  $\text{H}_2$ ,  $\text{CO}_2$ ,  $\text{H}_2\text{S}$  and  $\text{H}_2\text{Te}$  what is in complete accord with recent studies on modern terrestrial geothermal fields. Methods used comprise observations under binocular, optical and scanning electron microscope, and electron microprobe analysis.

**Keywords:** boiling; flowing flocs; electrum; adularia; hessite; greenockite; adularia-sericite deposits; low-sulfidation

---

## 1. Introduction

Exploration of active geothermal fields and epithermal deposits has revealed the formation of both vein adularia and platy calcite as originated from fluid becoming more alkaline due to the loss of acid volatiles during boiling of hydrothermal fluid. Boiling has been evidenced by the presence of coexisting liquid- and vapour-rich fluid inclusions in both minerals. These outcomes have made adularia and platy calcite to be mineral indicators of boiling [1–5]. They remain the only indicators of boiling when suitable fluid inclusions are lacking.

In this paper boiling is evidenced only by the presence of adularia and platy calcite since the present fluid inclusions are very small in size for investigation under optical microscope. The paper presents boiling assemblages in the Kupel occurrence, low-sulfidation epithermal Krumovgrad

goldfield and draws some conclusions about the impact of boiling for deposition of Au, Ag, Cu, Pb, Cd, and Te. Comparison with the next Khan Krum (known also as Ada Tepe) deposit is made as well.

The low-sulfidation epithermal Krumovgrad goldfield is located on the Eastern Rhodope Mountain, SE Bulgaria and in the eastern part of the Rhodope tectonic zone [6,7] and metallogenic province [8]. The Kupel occurrence is situated at c. 2 km to the SE of the well known Khan Krum deposit and has similar geological setting—hosted by supradetachment terrigenous rocks of the Shavar Formation (Maastrichtian-Paleocene) which are presented by breccias, breccia-conglomerates and sandstones originated from various metamorphic rocks. Movements along a regional low-angle detachment fault (Tokachka detachment) has implemented exhumation of deep metamorphic rocks from the core of Kessebir-Kardamos metamorphic dome (Figure 1) [9,10].

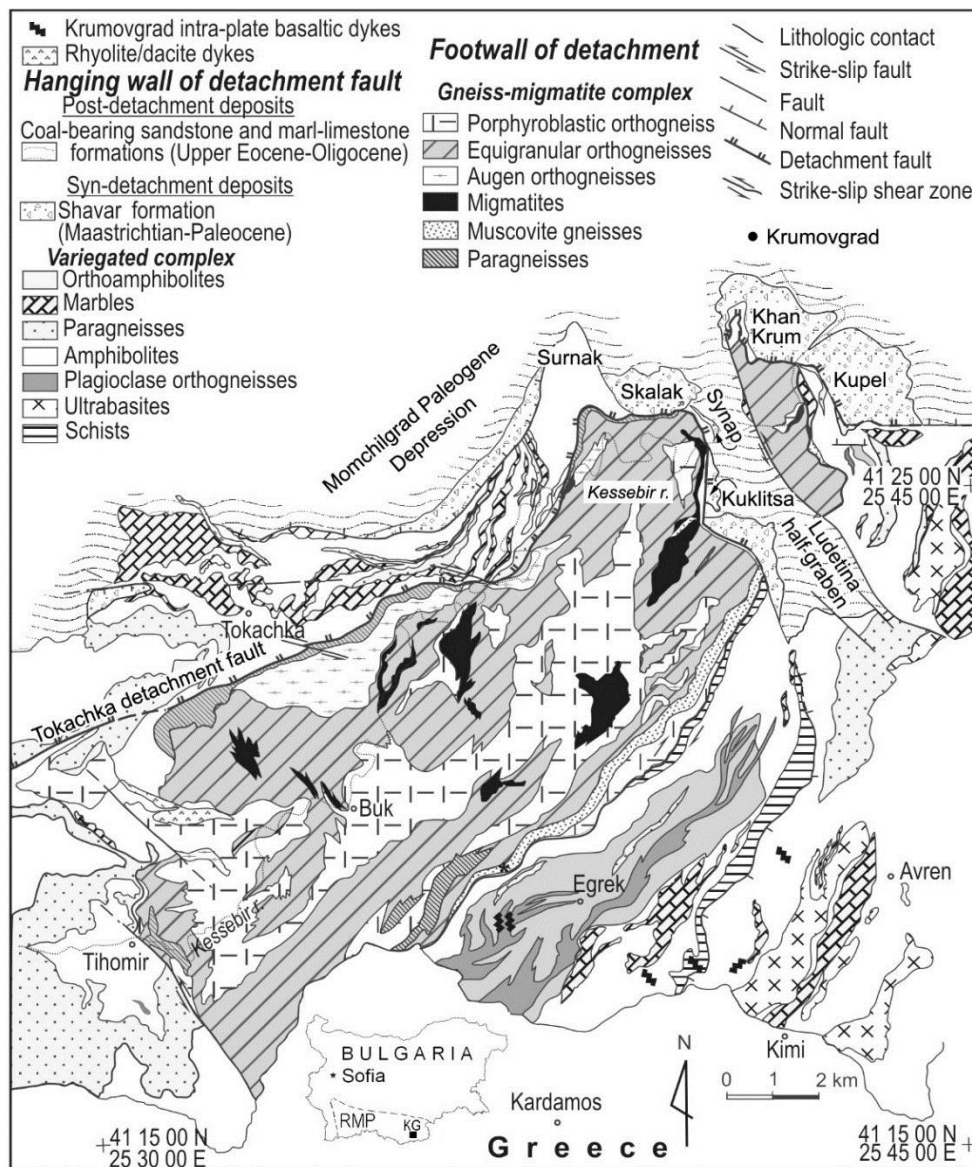


**Figure 1.** Geological map of the Kessebir-Kardamos metamorphic dome (after [9]; courtesy of P. Marchev) with added deposits and occurrences in the Krumovgrad goldfield as well the position of latter within Bulgarian territory. Contours of the Rhodope metallogenic province in Bulgaria are after [8]. *Abbr.:* RMP–Rhodope metallogenic province, KG–Krumovgrad goldfield.

## 2. Results and Discussion

Gold mineralization in the Kupel occurrence is hosted by grey fine-grained arkosic sandstones (Figure 2a) of grains smaller than 1 mm. The sandstones have formed at the expense of metamorphosed magmatic rocks of granodiorite composition. The first are composed mainly of angular to semi-rounded grains of quartz and feldspar, minor biotite and hornblende, and rare epidote, monazite, and titanite grains cemented by quartz and clays. The sandstones have undergone argillic, sericitic, pyritic (3 vol. %) and calcitic alterations (3–5 vol. %). Gold is observed mainly under microscope in quartz-adularia or calcite veinlets; in areas of dense cracking or disseminated in massive hydrothermal quartz. Auriferous veinlets cross-cut the sandstones and have similar dimensions: centimeter-scale length and thickness to a few millimeters (Figure 2).

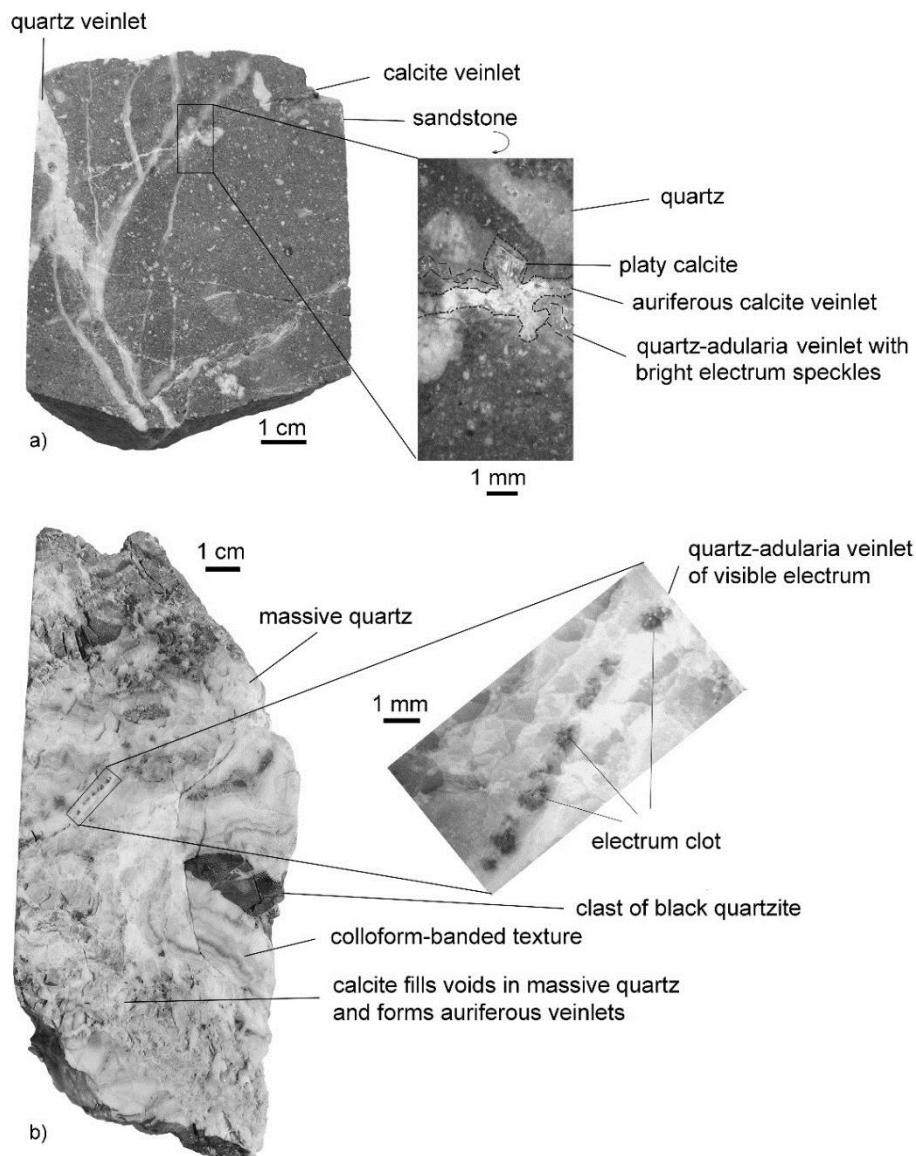


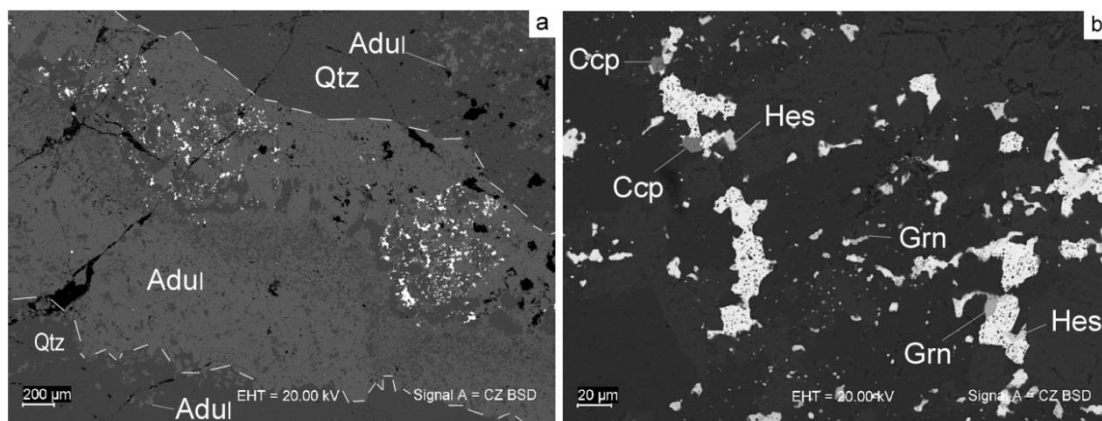
**Figure 2.** Borehole half cores from the Kupel occurrence (courtesy of DPMK): (a) Fine-grained sandstone is intersected by a network of quartz and calcite veinlets; inset–mirror image under stereomicroscope: quartz-adularia veinlet comprising bright electrum speckles is intersected by an auriferous veinlet of platy calcite. The margins of quartz and calcite veinlets are reinforced with black dotted lines for clearness; (b) Hydrothermal breccia is intersected by a millimeter-thick veinlet comprising visible electrum clots; inset under stereomicroscope–the veinlet containing visible electrum.

## 2.1. Boiling Assemblages

Boiling assemblages occur in two types of auriferous mineralization: veinlets of quartz-adularia, and of calcite composition (Figure 2). Boiling is evidenced by the presence of adularia and platy calcite; fluid inclusion evidence is not available since the present fluid inclusions are very small in size for investigation under optical microscope.

The auriferous quartz-adularia veinlets intersect massive hydrothermal quartz (Figure 2b). In the first the adularia abundances reach and even exceed 90 vol. % (Figure 3a) whereas in the second they reach up to 5 vol. %. In the quartz-adularia veinlets electrum appear as agglomerations, at places visible by naked eye whereas in the massive quartz it forms scarce grains visible only under optical microscope. The electrum agglomerations display globular shapes which reach 800  $\mu\text{m}$  across and are arranged along the veinlet length (Figure 2b and inset; Figure 3a). At higher magnifications of the scanning electron microscope details of the electrum paragenesis reveal: electrum is intergrown with chalcopyrite, galena, hessite and greenockite as the first prevails (Figure 3b,c). Hessite and greenockite appear also as small individual grains of a few microns across in the quartz-adularia matrix. Galena is observed in aggregates to about 30  $\mu\text{m}$  across, intergrown with electrum and hessite. It is worthy to say that sphalerite is absent. In cross-sections electrum aggregates display abundant silicate-filled pores of a few microns in size. The globular geometry of the electrum agglomerations, combined with their arrangement along the veinlet length, collectively suggest that these agglomerations likely were flowing particles. Their micron scale infers floc nature since the colloidal particles are much smaller.

In the Kupel occurrence the auriferous calcite veinlets are formed later than the auriferous quartz-adularia ones since the first clearly intersect the latter (Figure 2a, inset; Figure 3d–g). In other cases calcite has brecciated massive hydrothermal quartz (Figure 3g,h) what means that the fluid deposited calcite was overpressurized [11,12]. Calcite appears in lattice-bladed aggregates (Figure 3c). Electrum grains occupy boundaries between quartz and calcite grains; fills cracks in calcite and quartz (Figure 3e,f); and form accumulations in calcite veinlet portions of sharp thickness expansions after throttle portions which are barren (Figure 3g,h). The last situation displayed in Figure 3g,h demonstrates that the veinlet geometry has been first-order control on the electrum distribution and suggests that electrum has been transported by a flowing fluid, in a particulate form and deposited due to pressure drop during hydrofracturing. The electrum particles have been arrested in low velocity (expanded) portions of the ore conduits.



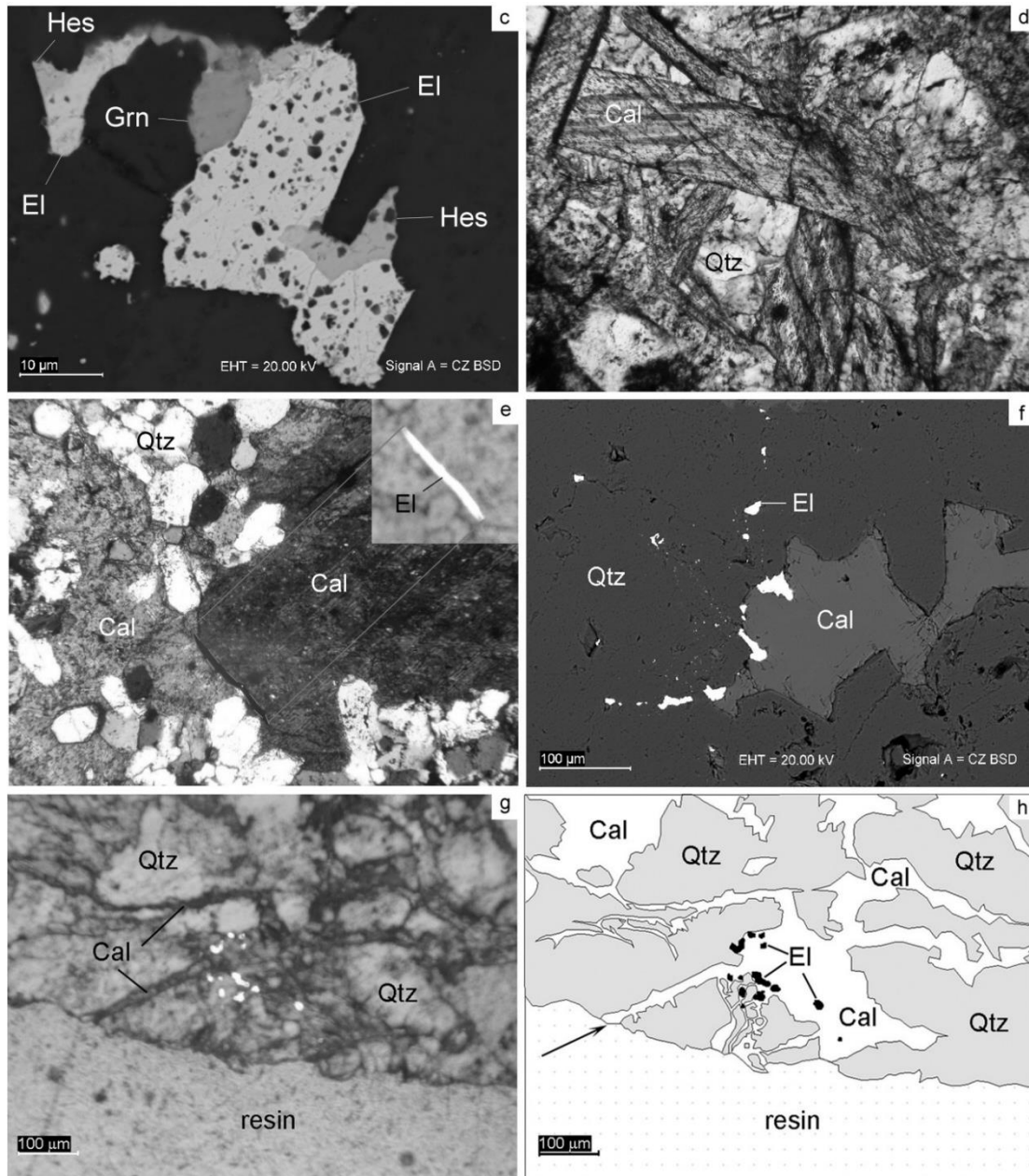


**Figure 3.** Auriferous veinlets: (a) Quartz-adularia veinlet from Figure 1a (the inset), scanning electron microscope (SEM). In the veinlet Adul>>Qtz, and electrum aggregates(bright) form globular shapes. In the host Qtz>>Adul. Veinlet boundaries are re-inforced with white dashed lines for clearness; (b) Enlarged view from “a” with intergrown electrum, hessite, chalcopyrite, galena and greenockite; (c) Enlarged view from the right bottom corner of “b”. Electrum displays highly porous texture in quartz-adularia matrix having pores filled with the matrix minerals; (d) Bladed calcite intersects hydrothermal quartz, plane polarized transmitted light; (e) Electrum wire deposited at calcite grain boundaries, plane polarized transmitted light. The inset displays the same electrum wire but in reflected light; (f) Chain of electrum grains along micro-cracks following in part a quartz-calcite interface, SEM; (g) Calcite veinlets filled open space in brecciated quartz; electrum highly accumulated in areas of sharp thickness expansion after throttle portions, cross polarized reflected light; (h) Drawing of “g”; arrow points the inferred flow direction. *Abbr.:* Qtz–quartz, Adul–adularia, El–electrum, Hes–hessite, Crn–greenockite, Gn–galena, Ccp–chalcopyrite, Cal–calcite, BSD–back scattered electrons.

## 2.2. Mineral Chemistry

- *Adularia*

- Adularia from electrum-rich quartz-adularia veinlets has entirely potassic composition without sodium (Table 1). In this it is identical to adularia from the Khan Krum and Kuklitsa deposits (unpublished data of the first author).

**Table 1.** Composition of adularia from the Kupel occurrence, wt %.

No.	Analysis No.	K <sub>2</sub> O	Na <sub>2</sub> O	Al <sub>2</sub> O <sub>3</sub>	SiO <sub>2</sub>	Sum
1	15	16.08	bdl	17.96	65.96	100.00
2	17	17.29	bdl	17.72	64.99	100.00
3	21	16.65	bdl	17.74	65.61	100.00

*Abbr.:* bdl–below detection limit.

- *Electrum*

- Composition of electrum from the two sorts of boiling assemblages is very similar according to the electron microprobe analysis (EPMA): electrum is composed of only gold and silver; no other constituents like copper are present (Table 2). Electrum from the Kupel occurrence (this study) in comparison with electrum from high-angle veins in the Khan Krum deposit [13] is enriched in gold and depleted in silver. The Au/Ag ratio of electrum in the Kupel is from 3.10 up to 3.50, whereas in the Khan Krum (outcrops on the summit) this ratio varies from 2.30 up to 3.2 but generally below 3. It is found that the gold enrichment in electrum increases with depth [14] or temperature [15–17]. These findings imply different levels of mineralization and/or formation temperature for the Kupel and Khan Krum with deeper level and/or higher temperature for the Kupel occurrence.

- *Hessite*

- Hessite is composed of only silver and tellurium (Table 3). Earlier, hessite associated with petzite (Ag<sub>3</sub>AuTe<sub>2</sub>), electrum, and galena has been found in the Khan Krum (Ada Tepe) deposit and reported in [9].
- Tellurides of gold and silver are constituents of epithermal both base metal ± Au-Ag and precious metal deposits, intrusion-related precious metal deposits as well as porphyry ones worldwide [18]. They display common relationship with calc-alkaline, subalkaline to alkaline igneous rocks [16,19–21]. In the Rhodopian section of the Alpine-Himalayan orogenic belt in Bulgaria and Greece they also occur in both epithermal base metal ± Au-Ag and precious metal deposits and in porphyry deposits [22]. In particular, in the Bulgarian section of the Rhodope metallogenic province Au-Ag tellurides have been found in Oligocene epithermal base metal (±gold) deposits like the Zvezdel-Pcheloyad orefield (hessite and calaverite [23,24]), Nedelino orefield (hessite and sulfotelluride [25,26]), Ardino deposit (hessite, Ag-sulfotelluride [27]), Davidkovo orefield (hessite, cervelleite and Ag<sub>4</sub>TeS<sub>2</sub> [28,29]), Enyovche deposit (cervelleite [30]) and, as mentioned above, in the Eocene epithermal Khan Krum (Ada tepe) gold deposit (hessite and petzite [9]). Some of these orefields and deposits like Davidkovo and Nedelino orefields, and Ardino and Enyovche deposits do not display relationship with particular magmatism since coeval large magmatic intrusions are not exposed but only felsic dykes. Despite this absence, that relationship is suspected based on deposit's geochemical signature or isotopic ages [9,31–33]. In the Greek section of the Rhodope metallogenic province porphyry and epithermal high- to intermediate-sulfidation precious metal deposits contain significant amounts of Au-Ag tellurides including hessite and sulfotellurides. These Greek deposits display clear relationship with calc-alkaline, high-K calc-alkaline to shoshonitic intrusive rocks [20].

**Table 2.** Composition of electrum from the Kupel occurrence, wt %.

No.	Analysis No.	Boiling Assemblage	Au	Ag	Sum	Au/Ag
1	1	El-Qtz-Adul-Sul-Tel	77.44	22.56	100.00	3.43
2	2	El-Qtz-Adul-Sul-Tel	76.24	23.76	100.00	3.21
3	3	El-Qtz-Adul-Sul-Tel	77.03	22.97	100.00	3.35
4	4	El-Qtz-Adul-Sul-Tel	76.87	23.13	100.00	3.32
5	5	El-Qtz-Adul-Sul-Tel	76.15	23.85	100.00	3.19
6	6	El-Qtz-Adul-Sul-Tel	76.81	23.19	100.00	3.31
7	7	El-Qtz-Adul-Sul-Tel	76.35	23.65	100.00	3.23
8	8	El-Qtz-Adul-Sul-Tel	75.63	24.37	100.00	3.10
9	9	El-Qtz-Adul-Sul-Tel	76.13	23.87	100.00	3.19
10	10	El-Qtz-Adul-Sul-Tel	76.15	23.85	100.00	3.19
11	11	El-Qtz-Adul-Sul-Tel	76.31	23.69	100.00	3.22
12	12	El-Qtz-Adul-Sul-Tel	77.46	22.54	100.00	3.44
13	13	El-Qtz-Cal	77.00	23.00	100.00	3.35
14	14	El-Qtz-Cal	77.77	22.23	100.00	3.50
15	16	El-Qtz-Cal	77.48	22.52	100.00	3.44
16	18	El-Qtz-Cal	76.41	23.59	100.00	3.24
17	19	El-Qtz-Cal	76.69	23.31	100.00	3.29
18	20	El-Qtz-Cal	76.63	23.37	100.00	3.28
19	30	El-Qtz-Cal	80.60	19.40	100.00	4.15

Abbr.: El–electrum, Qtz–quartz, Adul–adularia, Sul–sulfides, Tel–tellurides, Cal–calcite.

- For the Krumovgrad goldfield the relationship between precious metal mineralization–magmatism remains unclear. The goldfield is older ( $35 \pm 0.2$  Ma Ar/Ar age of adularia) [9]) than the near-by Iran Tepe volcano ( $\sim 33.9$  Ma for the oldest lava flow) [34] which is the oldest Tertiary volcano in the Eastern Rhodope Mountain [35,36]. That still maintains a question about the origin of the Krumovgrad goldfield.
- Au-Ag tellurides deposit usually at low temperature in the range of 280–200 °C; for instance, at 250–200 °C [37–39]; below 260 °C [28]; at 280–240 °C [21]. These data are in line with the temperature of deposition of the gold-silver mineralization in the next Ada tepe (Khan Krum) deposit (250–220 °C) [40]. The deposition of Au-Ag tellurides is constrained in other similar low-sulfidation precious metal deposits to occur under neutral to slightly acid conditions [21,38,41]. These data allow one to conclude that hessite in the Kupel occurrence constrains low temperature and neutral to slightly acid conditions.
- *Greenockite*
  - Greenockite is found for the first time in the Krumovgrad goldfield in this study. It contains small amounts of Zn and Fe (Table 3).
  - Greenockite is a rare mineral in the Earth. It is mainly known as present in base metal deposits worldwide in close association with sphalerite/wurtzite [42]. The same holds for the Bulgarian deposits: it is found in the stratiform base metal Sedmochislenitsi deposit hosted by Triassic lime- and dolostones, in the Oligocene Madan base metal orefield, Central Rhodope, hosted by Pre-Paleocene high-grade metamorphic rocks [43], and in the Oligocene Madzharovo base metal + gold orefield [44] hosted by Oligocene shoshonitic volcanic rocks [33]. Other less known occurrences of greenockite appear epithermal Au-Ag ± base metal deposits, for instance Cirotan, Yava, Indonesia hosted by rhyolites, dacites, and quartz microdiorite [45,46]; La Guitarra, Mexico hosted by monzogranite and granitic dykes [14]; Tinos island, Greece in spatial proximity of Tinos granodiorite to leucogranite pluton [47]; Costa Rica hosted by andesites and basalts [48]. Greenockite is also found as a sublimate in volcanic gasses in the circum-Pacific Fire Rim intergrown or associated with

cadmium-bearing sulfosalts [49,50]. Hydrothermal hypogene greenockite is commonly reported as a late, low-temperature mineral. In the Madzharovo base metal + gold orefield greenockite has deposited during the late auriferous quartz-chalcedony-sulfalt stage at 220–180 °C [51]. In Cirotan greenockite has formed at c. 250 °C during lowering the sulfur activity and increasing the Te one, from neutral, low-salinity fluid [45,46]. In the Tinos island, greenockite and zincian greenockite have deposited under hydrostatic pressure at about 200 °C [47]. In Costa Rica the epithermal mineralization including electrum and greenockite has formed between 290 and 180 °C from low-salinity fluids [48]. These data are in accord with the temperature of deposition and low salinity origin of the gold-silver mineralization in the next Ada tepe deposit (250–220 °C) [40] and infer similar temperature range and low-salinity fluid also for the Kupel occurrence.

**Table 3.** Representative electron microprobe analyses of minerals intergrown with electrum, wt %.

Mineral	Hess	Hess	Hess	Hess	Hess	Hess	Grn	Grn	Grn	Gn	Gn
An. No.	23	24	25	26	29	35	26	27	32	32	35
Au	bdl										
Ag	61.77	61.68	61.86	61.86	61.81	60.97	bdl	bdl	bdl	bdl	bdl
Pb	bdl	87.26	87.54								
Cu	bdl										
Cd	bdl	bdl	bdl	bdl	bdl	bdl	78.03	81.90	76.36	bdl	bdl
Fe	bdl	bdl	bdl	bdl	bdl	bdl	0.34	bdl	bdl	bdl	bdl
Zn	bdl	bdl	bdl	bdl	bdl	bdl	3.43	bdl	3.50	bdl	bdl
S	bdl	bdl	bdl	bdl	bdl	bdl	20.20	18.10	20.14	12.74	12.46
Te	38.13	38.23	38.06	38.14	38.19	39.03	bdl	bdl	bdl	bdl	bdl
Sum	100.00	100.00	100.00	100.00	100.00	100.00	100.00	100.00	100.00	100.00	100.00

*Abbr.:* Hess–hessite, Grn–greenockite, Gn–galena, btl–below detection limit.

- *Galena*
  - Galena is composed of only lead and sulphur (Table 3).

### 2.3. Significance of Throttling

High accumulation of electrum after throttle portions has already been described in samples from the next Khan Krum deposit in [52]. That picture has been interpreted with a causative sequence of several processes: (i) increased boiling in expanded veinlet portions compared to weak boiling or non-boiling conditions in narrow ones; (ii) flocculation of colloidal solution and retention/arrest of heavy electrum flocs in expanded veinlet portions (low velocity zones) and (iii) formation of mixed electrum-silicate gel and its further crystallization. Earlier, numerical simulations have demonstrated that throttling leads to “cessation of boiling” [53]. These authors have inferred stopping of the gold deposition in throttle portions of ore conduits. Accumulations of precious and base metals has been found downstream of throttles installed in geothermal production wells in New Zealand for a pressure reduction of the geothermal fluid [54]. Formation of colloidal solution as a response to boiling has been proposed in other studies of epithermal deposits and geothermal systems [55–58].

### 2.4. Boiling and Deposition of Au, Ag, Cu, Pb, Cd and Te

The assemblages in the Kupel occurrence besides boiling indicate in addition a saturation of hydrothermal fluid in respect to their minerals and hence high effectiveness of boiling for deposition of Au, Ag, Cu, Pb, Cd and Te through collective loss of H<sub>2</sub>, CO<sub>2</sub>, H<sub>2</sub>S and H<sub>2</sub>Te. Similarly, in [59] it have been concluded that boiling removes the same metals from geothermal solutions. In contrast, other elements like Zn only partially remove during boiling and remain available for transport and deposition in peripheral and shallow portions of an epithermal system [59]. The absence of sphalerite demonstrated in this study is in line with the conclusion in [59] about the behavior of Zn during boiling. The significance of boiling as a key control on the deposition of tellurides, Te-rich sulfides

and sulfosalts in epithermal Au-Ag-Te deposits has also been proposed in [37,60]. In addition, particulate form of sulfides and tellurides before deposition in sulfide-telluride-rich vein bands has been underlined in [37].

As shown above, the Kupel occurrence with its presence of tellurides is analogous to the next Khan Krum deposit but some differences occur: (i) electrum in the Kupel occurrence is richer in gold than that of the Khan Krum deposit and (ii) greenockite has not been found in the Khan Krum deposit.

### *2.5. Possible Sources of Te*

The presence of Au-Ag tellurides in the precious metal mineralization of Krumovgrad goldfield and their genetic relationship with calc-alkaline to alkaline rocks, well constrained in the literature, suggest a relationship of the goldfield with underlying shallow calc-alkaline and high-K intrusive rocks. Two available contributors of Te exist in the Kessebir-Kardamos dome where the supradetachment terrigenous rocks host the precious metal mineralization: (i) Te-bearing magmatic fluids separated from shallow seated and buried plutons of Eocene age and (ii) leaching of Te from the older metamorphic rocks in the core of the metamorphic dome.

The first possibility is advocated in [9,13]. The authors of [9] have proposed that volcanism in the Eastern Rhodope has been preceded by an accumulation of magma at greater depths. Lately, it has been suggested that the Eastern Rhodope gold deposits have been related to intrusions of deep-seated mafic magmas [61]. The first author of the present study thinks that such mafic rocks should be parental of both epithermal mineralization and Iran Tepe volcano since the volcanic rocks of the latter bear calc-alkaline and high-K characteristics [34]. The second possibility exists because of the presence of old intrusive rocks of similar high-K characteristics in depth. The metamorphic core complexes of the Rhodope Tectonic zone comprise metamorphosed I- and S-granitoids of Palaeozoic to Mesozoic age which have originated from the crust or enriched subcontinental mantle and crust [62]. In the core of Byala Reka metamorphic dome, next to the East, there are also granitoids [63]. The core granitoids fall into the field of high-K calc-alkaline and K-subalkaline rocks [64]. To constrain the source of Te for the tellurides in the Krumovgrad goldfield a sampling of the Rhodope metamorphic basement and determination of the Te abundances in the different metamorphic rocks are required in future.

## **3. Materials and Methods**

The studied samples comes from borehole cores provided by Dundee Precious Metals Krumovgrad Co. (DPMK). The methods comprise observations under stereo and optical microscope (in transmitted and reflected light), scanning electron microscope, and electron microprobe analysis. Mineral composition was defined in polished sections from borehole cores using energy dispersive X-ray microprobe analysis through ZEISS SEM EVO 25 LS-EDAX Tident spectrometer at acceleration voltage of 15 kV, electron beam current of 500 pA and beam diameter of 1  $\mu\text{m}$  for all analyses. The standardless quantification results are performed through automatic background subtraction, matrix correction, and normalization to 100% for all of the elements in the peak identification list. Data from EMPA in the tables are from individual point analyses with detection limits <0.01 wt %.

## **4. Conclusions**

1. Precious metal mineralization in the Kupel occurrence, Krumovgrad goldfield, is presented mainly by electrum and trace hessite, chalcopyrite, galena, and greenockite. It has deposited in a response of multiple boiling episodes resulted from hydrofracturing by overpressurized fluid. The boiling is evidenced by the presence of vein adularia and platy calcite and it demonstrates high effectiveness for deposition of Au, Ag, Cu, Pb, Cd and Te.
2. Two types of boiling assemblages and respective two ore stages were identified: (i) earlier, quartz-adularia-electrum-chalcopyrite-galena-hessite-greenockite and (ii) later, calcite-electrum

- one. The first assemblage displays textural evidence for flocculation of colloidal solution of silicates and electrum like in the next Khan Krum deposit. The second assemblage is specific for the Kupel occurrence and increases its gold potential.
3. The higher gold content in electrum from the Kupel occurrence compared to the one from the next Khan Krum deposit as well as the presence of greenockite in the first both suggest deeper level and/or higher formation temperature for the Kupel occurrence.
  4. The presence of tellurides in the Krumovgrad goldfield and their relationship with calc-alkaline, subalkaline and alkaline rocks worldwide, points to two possible sources: (i) underlying shallow calc-alkaline and high-K Eocene intrusive rocks through magma degassing or (ii) metal leaching from host metagranitoid rocks by hot fluids. Tellurides points also to a formation temperature in the range of 280–200 °C and origin from neutral to slightly acid, low-salinity fluids.

**Acknowledgments:** The authors thank DPMK for provided borehole cores and permission to publish. Thanks are due to P. Ivanova (IMC) for petrographic investigation of sandstone.

**Author Contributions:** I.M. performed the optical observations and wrote the paper; E.T. performed the EMPA, took the SEM images, and described the respective methods.

**Conflicts of Interest:** The authors declare no conflict of interest. DPMK has given permission to publish the results.

## Abbreviations

The following abbreviations are used in this manuscript:

RMP	Rhodope metallogenic province
KG	Krumovgrad goldfield
SEM	scanning electron microscope
DPMK	Dundee Precious Metals Krumovgrad
Adul	adularia
Qtz	quartz
El	electrum
Hes	hessite
Crn	greenockite
Gn	galena
Ccp	chalcopyrite
Cal	calcite
BSD	back scattered electrons
bdl	below detection limit
EPMA	electron microprobe analysis
Sul	sulfides
Tel	tellurides

## References

1. Browne, P.R.L. Hydrothermal alteration in active geothermal fields. *Ann. Rev. Earth Planet Sci.* **1978**, *6*, 229–250.
2. Henley, R.W. The geothermal framework of epithermal deposits. In *Geology and Geochemistry of Epithermal Deposits*; Berger, B.P., Bethke, P.M., Eds; Reviews in Economic Geology: 1985; Volume 2, pp. 1–24.
3. Henley, R.W. Epithermal gold deposits in volcanic terranes. In *Gold Metallogeny and Exploration*; Foster, R.R., Ed.; Chapman & Hall: London, UK, 1993; pp. 133–163.
4. Simmons, S.F.; Christenson, B.W. Origins of Calcite in a Boiling Geothermal System. *Am. J. Sci.* **1994**, *294*, 361–400.
5. Dong, G.; Morrison, G. Adularia in epithermal veins, Queensland: Morphology, structural state and origin. *Miner. Depos.* **1995**, *30*, 11–19.
6. Nachev, I.; Nachev, C. *Alpine Plate-Tectonics of Bulgaria*; Artik: Sofia, Bulgaria, 2001; 198p.

7. Bonev, N.; Spikings, R.; Moritz, R.; Marchev, P.; Collings, D.  $^{40}\text{Ar}/^{39}\text{Ar}$  age constraints on the timing of Tertiary crustal extension and its temporal relation to ore-forming and magmatic processes in the Eastern Rhodope Massif, Bulgaria. *Lithos* **2013**, *180–181*, 264–278.
8. Georgiev, V. Metallogenic map of gold deposits in Bulgaria. In *Gold Deposits of Bulgaria*; Milev, V., Ed.; Zemya'93: Sofia, Bulgaria, 2007. (In Bulgarian with summary in English).
9. Marchev, P.; Singer, B.; Jelev, D.; Hasson, S.; Moritz, R.; Bonev, N. The Ada Tepe deposit: A sediment-hosted, detachment fault-controlled, low-sulfidation gold deposit in the Eastern Rhodopes, SE Bulgaria. *Schweiz. Mineral. Petrogr. Mitt.* **2004**, *84*, 59–78.
10. Márton, I.; Jeleva, T.; Dintchev, Y.; Zhivkov, N.; Gosse, R. Sedimentary Rock-Hosted Gold Mineralization at Ada Tepe, Krumovgrad District, Bulgaria: Review of Prospect-Scale Geological, Structural and Geochemical Features. In *Eocene to Miocene Hydrothermal Deposits of Northern Greece and Bulgaria: Relationships between Tectonic-Magmatic Activity, Alteration, and Gold Mineralization. Guidebook Series, Field Trip (Balkans II)*; Voudouris, P., Siren, C.R., Márton, I., Eds.; Society of Economic Geologists: Littleton, CO, USA, 2016; Volume 54, pp. 17–42.
11. Chi, G.; Xue, C. An overview of hydrodynamic studies of mineralization. *Geosci. Front.* **2011**, *2*, 423–438.
12. Bons, P.; Fusswinkel, T.; Gomez-Rivas, E.; Markl, G.; Wagner, T.; Walter, B. Fluid mixing from below in unconformity-related hydrothermal ore deposits. *Geology* **2014**, *42*, 1035–1038.
13. Marinova, I.; Ganev, V.; Titorenkova, R. Colloidal origin of colloform-banded textures in the Paleogene low-sulfidation Khan Krum gold deposit, SE Bulgaria. *Miner. Depos.* **2014**, *49*, 49–74.
14. Camprubi, A.; Ganais, A.; Gardellach, E.; Prol-Ledesma, R.M.; Rivera, R. The La Guitarra Ag-Au Low-Sulfidation Epithermal Deposit, Temascaltepec District, Mexico: Vein Structure, Mineralogy, and Sulfide-Sulfosalt Chemistry. *Soc. Econ. Geol.* **2001**, *SP8*, 133–158.
15. Shikazono, N.; Shimizu, M. Compositional Variations in Au-Ag Series Mineral from Some Gold Deposits in the Korean Peninsula. *Min. Geol.* **1986**, *36*, 545–553.
16. Plotinskaya, O.; Kovalenker, V.; Seltmann, R.; Stanley, C. Te and Se mineralogy of the high-sulfidation Kochbulak and Kairagach epithermal gold telluride deposits (Kurama Ridge, Middle Tien Shan, Uzbekistan). *Mineral. Petrol.* **2006**, *87*, 187–207.
17. Pal'yanova G. Physicochemical modeling of the coupled behavior of gold and silver in hydrothermal processes: Gold fineness, Au/Ag ratios and their possible implications. *Chem. Geol.* **2008**, *255*, 399–413.
18. Cook, N.; Ciobanu, C.; Spry, P.; Vouvouris, P. Understanding gold-(silver)-telluride-(selenide) mineral deposits. *Episodes* **2009**, *32*, 249–263.
19. Pals, D.W.; Spry, P.G. Telluride mineralogy of the low-sulfidation epithermal Emperor gold deposit, Vatukoula, Fiji. *Mineral. Petrol.* **2003**, *79*, 285–307.
20. Voudouris, P. A comparative mineralogical study of Te-rich magmatic-hydrothermal systems in northeastern Greece. *Mineral. Petrol.* **2006**, *87*, 241–275.
21. Zhai, D.; Liu, J. Gold-telluride-sulfide association in the Sandaowanzi epithermal Au-Ag-Te deposit, NE China: Implications for phase equilibrium and physicochemical conditions. *Mineral. Petrol.* **2014**, *108*, 853–871.
22. Kostov-Kytin, V.; Kostov, R.I.; Ivanova, P. The electronic bibliographic data base on minerals from Bulgaria: Actual state, potentialities, and perspectives. *Rev. Bulg. Geol. Soc.* **2013**, *74*, 111–130.
23. Atanasov, V.; Breskovska, V. Sulfosalts from the Zvezdel Ore District and their mineral paragenesis. *Annuaire de l'Univ. de Sofia* **1964**, *57*, 197–204. (In Bulgarian)
24. Mladenova, V. Mineralogy of the Eseler deposit, Zvezdel-Pcheloyad orefield. *Annuaire de l'Univ. de Sofia* **1984**, *78*, 354–373. (In Bulgarian)
25. Gadzheva, T.I. Tellurides from the Shadiitsa deposit, Central Rhodope. *Comptes Rendus Bulg. Acad. Sci.* **1983**, *36*, 245–247. (In Bulgarian)
26. Gadzheva, T.I. The (Ag, Cu) $_4$ TeS mineral from the Shadiitsa deposit, Central Rhodope. *Comptes Rendus Bulg. Acad. Sci.* **1985**, *38*, 211–213. (In Bulgarian)
27. Bonev, I. Mineralogy and geochemistry of the Ardino polymetallic deposit. *Geochem. Mineral. Petrol.* **1991**, *27*, 25–62 (in Bulgarian).
28. Marinova, I. Mineralogy and Geochemistry of Lead-Zinc Deposits of the Davidkovo Orefield, Central Rhodope. Ph.D. Thesis, Sofia University, Sofia, Bulgaria, 1994. (In Bulgarian)

29. Marinova, I.; Kolkovski, B. New data on mineralization sequence and mineralogy of the Davidkovo orefield, Central Rhodopes. *Annuaire de l'Univ. de Sofia* **1994**, *84*, 301–343. (In Bulgarian with summary in English)
30. Dobrev, S.; Strashimirov, S.; Vasileva, M.; Dragiev, H. Silver and silver-bearing minerals from the Chala and Pcheloyad deposits (Eastern Rhodope) and from the Enyovche deposit (Central Eastern Rhodope). *Annu. Univ. Min. Geol. "St. Ivan Rilski"* **2001**, *45*, 41–47 (In Bulgarian)
31. Kolkovski, B.; Manev, D. Madan orefield. In *Lead-Zinc Deposits of Bulgaria*; Dimitrov, R., Ed.: Tehnika: Sofia, Bulgaria, 1988, 37–64.
32. Marinova, I. Chemical composition of the lead-zinc deposits in Davidkovo orefield, Central Rhodopes–complexity and regularities. *Annuaire de l'Univ. de Sofia* **1995**, *88*, 169–177.
33. Marchev, P.; Kaiser-Rohmeier, M.; Heinrich, C.; Ovcharova, M.; von Quadt, A.; Raicheva, R. Hydrothermal ore deposits related to post-orogenic extensional magmatism and core complex formation: The Rhodope Massif of Bulgaria and Greece. *Ore Geol. Rev.* **2005**, *27*, 53–89.
34. Marchev, P.; Kibarov, P.; Spikings, R.; Ovtcharova, M.; Márton, I.; Moritz, R. <sup>40</sup>Ar/<sup>39</sup>Ar and U-Pb geochronology of the Iran Tepe volcanic complex, Eastern Rhodopes. *Geol. Balc.* **2010**, *39*, 3–12.
35. Ivanov, R. Magmatism in the EastRhodopian Paleogene depression. Part 1–Geology. *Trudove Varhu Geologiatata na Balgaria* **1960**, *1*, 311–383. (In Bulgarian with summary in Russian)
36. Goranov, A. Lithology of Paleogene deposits in part of Eastern Rhodope. *Trudove Varhu Geologiatata na Balgaria* **1960**, *1*, 259–310. (In Bulgarian with summary in German)
37. Ahmad, A.; Solomon, M.; Walshe, J.L. Mineralogical and geochemical Studies of the Emperor Gold Telluride Deposit, Fiji. *Econ. Geol.* **1987**, *82*, 345–370.
38. Tombros, S.; Seymour, K.; Spry, P.; Williams-Jones, A.; Zouzias, D. Panormos Bay Au-Ag-Te epithermal mineralization, Tinos island, Hellas: Multiple mechanisms of deposition for an unusual calc-alkaline granite related system. In Proceedings of the International Earth Sciences Colloquium on the Egean Regions, Izmir, Turkey, 4–7 October 2005; pp. 326–334.
39. Kovalenker, V.A.; Plotinskaya, O.Y. Te and Se mineralogy of Ozernovskoe and Prasolovskoe epithermal gold deposits (Kuril–Kamchatka volcanic belt). *Geochem. Mineral. Petrol.* **2005**, *43*, 118–124.
40. Márton, I.; Moritz, R.; Marchev, P.; Vennemann, T.; Spangenberg, J. Fluid Evolution Within Eastern Rhodopian Sedimentary Rock-hosted Low-sulfidation Epithermal Gold Deposits, Bulgaria. In Proceedings of the 2006 IGCP-486 Field Workshop, Izmir, Turkey, 24–29 September 2006; Cook, N.; Özgenc, I.; Oyman, T.; Eds.; pp. 116–123.
41. Scherbarth, N.; Spry, P. Mineralogical, Petrological, Stable Isotope, and Fluid Inclusion Characteristics of the Tuvatu Gold-Silver Telluride Deposit, Fiji: Comparisons with the Emperor Deposit. *Econ. Geol.* **2006**, *101*, 135–158.
42. Schwartz, M. Cadmium in Zinc Deposits: Economic Geology of a Polluting Element. *Int. Geol. Rev.* **2000**, *42*, 445–469.
43. Kostov, I.; Breskovska, V.; Mincheva-Stefanova, Y.; Kirov, G. *Minerals in Bulgaria*; Marin Drinov Acad. Publisher: Sofia, Bulgaria, 1964; p. 540.
44. Tarkian, M.; Breskovska, V. Greenockite from the Madjarovo Pb-Zn Ore District, Eastern Rhodope, Bulgaria. *Mineral. Petrol.* **1989**, *40*, 137–144.
45. Marcoux, E.; Milesi, J.-P.; Sohearto, S.; Rinawan, R. Noteworthy mineralogy of the Au-Ag-Sn-W(Bi) epithermal ore deposit of Cirotan, West Java, Indonesia. *Can. Mineral.* **1993**, *31*, 727–744.
46. Yuningsih, E.T.; Matsueda, H.; Rosana, M.F. Epithermal Gold-Silver Deposits in Western Java, Indonesia: Gold-Silver Selenide-Telluride Mineralization. *Indones. J. Geosci.* **2014**, *1*, 71–81.
47. Tombros, S.; Seymour, K.; Spry, P.; Williams-Jones, A. Greenockite and zincian greenockite in epithermal polymetallic Ag-Au-Te mineralization, Tinos Island, Hellas: Description and conditions of formation. *Neues Jahrb. Mineral. Abh.* **2005**, *182*, 1–9.
48. Mixa, P.; Dobesh, P.; Zachek, V.; Lukesh, P.; Quintanilla, E. Epithermal gold mineralization in Costa Rica, Cordillera de Tilarán–exploration geochemistry and genesis of gold deposits. *J. Geosci.* **2011**, *56*, 81–104.
49. Chaplygin, I.; Mozgova, N.; Magazina, L.; Kuznetsova, O.; Safonov, Y.; Bryzgalov, I.; Makovicky, E. Kudriavite, (Cd, Pb)Bi<sub>2</sub>S<sub>4</sub>, A New mineral species from Kudriavy volcano, Iturup island, Kurile arc, Russia. *Can. Mineral.* **2005**, *43*, 695–701.

50. Zelenski, M.; Bortnikova, S. Sublimate speciation at Mutnovsky volcano, Kamchatka. *Eur. J. Mineral.* **2005**, *17*, 107–118.
51. Breskovska, V.; Gergelchev, V. Madzharovo orefield. In *Lead-Zinc Deposits of Bulgaria*; Dimitrov, R., Ed.; Tehnika: Sofia, Bulgaria, 1988; pp. 114–127. (In Bulgarian with abstract in Russian and English)
52. Marinova, I. Particular Distribution of Electrum Enrichments along Sinusoidal-Walled Veinlets and Geological Implications: A Case Study from the Eocene Low-Sulfidation Khan Krum Deposit, SE Bulgaria. In *Horizons Earth Science Research*; Veress, B., Szegethy, J., Eds.; Nova Science Publ.: New York, NY, USA, 2017; Volume 16, pp. 121–155.
53. Cooke, D.; McPhail, D. Epithermal Au-Ag-Te Mineralization, Acupan, Baguio District, Philippines: Numerical Simulations of Mineral Deposition. *Econ. Geol.* **2001**, *96*, 109–131.
54. Browne, K.L. Gold deposition from geothermal discharges in New Zealand. *Econ. Geol.* **1986**, *81*, 979–983.
55. Saunders, J.A. Colloidal transport of gold and silica in epithermal precious-metal systems: Evidence from the Sleeper deposit, Nevada. *Geology* **1990**, *18*, 757–760.
56. Saunders, J.A. Silica and gold textures in bonanza ores of the Sleeper deposit, Humboldt County, Nevada: Evidence for colloids and implications for epithermal ore-forming process. *Econ. Geol.* **1994**, *89*, 628–638.
57. Saunders, J.; Schoenly, P. Boiling, colloid nucleation and aggregation, and the genesis of bonanza Au-Ag ores of the Sleeper deposit, Nevada. *Miner. Depos.* **1995**, *30*, 199–210.
58. Gartman, A.; Hannington, M.; Jamieson, J.; Peterkin, B.; Garbe-Schonberg, D.; Findlay, A.; Fuchs, S.; Kwasnietzka, T. Boiling-induced formation of colloidal gold in black smoker hydrothermal fluids. *Geology* **2017**, *46*, 39–42.
59. Simmons, S.F.; Brown, K.L.; Tutolo, B.M. Hydrothermal Transport of Ag, Au, Cu, Pb, Te, Zn, and Other Metals and Metalloids in New Zealand Geothermal Systems: Spatial Patterns, Fluid-Mineral Equilibria, and Implications for Epithermal Mineralization. *Econ. Geol.* **2016**, *111*, 589–618.
60. Tombros, S.; Seymour, K.; Williams-Jones, A. Controls on Tellurium in Base, Precious, and Telluride Minerals in the Panormos Bay Ag-Au-Te Deposits, Tinos Island, Cyclades, Greece. *Econ. Geol.* **2010**, *105*, 1097–1111.
61. Marchev, P.; Arai, S.; Vaselli, O. Cumulate xenoliths in Oligocene alkaline basaltic and lamprophyric dykes from the eastern Rhodopes, Bulgaria: Evidence for the existence of layered plutons under the metamorphic core complexes. *Geol. Soc. Am.* **2006**, *409*, 237–258.
62. Ovcharova, M. Petrology, Geochronology and Isotopic Studies on Metagranitoids from the Eastern Part of the Madan-Davidkovo Swell. Ph.D. Thesis-Sofia University, Sofia, Bulgaria, 2005. (In Bulgarian)
63. Macheva, L.; Kolcheva, K. Metagranitoids from Eastern Rodopes—occurrences and main features. *Comptes Rendus Bulg. Acad. Sci.* **1992**, *45*, 63–66.
64. Ovcharova, M.; Sarov, S. Petrology and tectonic setting of the metagranitoids from Kesibir Reka region in the Eastern Rhodopes. *Geol. Soc. Greece* **1995**, *4*, 613–618.



© 2018 by the authors; licensee MDPI, Basel, Switzerland. This article is an open access article distributed under the terms and conditions of the Creative Commons by Attribution (CC-BY) license (<http://creativecommons.org/licenses/by/4.0/>).